We have already presented experimental results on the transfer inefficiency ϵ as a function of clock frequency f [5]. It can be seen that ln (α) increases linearly with the increase of ln (f) at higher frequencies. This agrees with the analysis described above. From the experimental linear characteristics of ln (ϵ) versus ln (f) at higher frequencies, we obtain 510 K as the value of T_G. The ϵ at lower frequencies also increases with the decrease of clock frequency. This is considered to be caused by leakage current.

IV. Conclusion

When analyzing a-Si device operations the localized states must be taken into account, because a-Si has so many localized states in the band gap. In this paper, the transfer inefficiency of a-Si CCD's is evaluated numerically and analytically on the basis of the assumption that the localized states in a-Si are distributed exponentially with respect to energy. We have clarified that ln (ϵ) versus ln (f) is linear and that its coefficient is determined by T_G and T. This feature agreed with our experimental results. And since the rate equation and the conservation equation used in this analysis can be applied to the a-Si FET's this analysis is considered applicable for the design and analysis not only of a-Si CCD's but also of a-Si FET's.

References

[1] P. G. LeComber, W. E. Spear, and A. Ghaith, "Amorphous-silicon field-effect device and possible application," *Electron. Lett.*, vol. 15, pp. 179-181, 1979.

[2] A. J. Snell, K. D. Mackenzine, W. E. Spear, P. G. LeComber, and A. J. Hughes, "Application of amorphous silicon field effect transistors in addressable liquid crystal display panels," *Appl. Phys.*, vol. 24, pp. 357-362, 1981.

[3] M. Matsumura, H. Hayama, Y. Nara, and K. Ishibashi, "Amorphous-silicon image sensor IC," *IEEE Electron Device Lett.*, vol. EDL-1, pp. 182-184, 1980.

[4] K. Ishibashi and M. Matsumura, "Amorphous-silicon/silicon-oxynitride field-effect transistors," *Appl. Phys. Lett.*, vol. 41, pp. 454-456, 1982.

[5] S. Kishida, Y. Nara, O. Kobayashi, and M. Matsumura, "Amorphous-silicon charge-coupled devices," *Appl. Phys. Lett.*, vol. 41, pp. 1154-1156, 1982.

[6] M. F. Tompsett, "The quantitative effects of interface states on the performance of charge-coupled devices," *IEEE Trans. Electron Devices*, vol. ED-20, pp. 45-55, 1973.

[7] O. Sugiura and M. Matsumura, "Control of a-Si FETs' characteristics by impurity-doping," *Trans. IECE Japan*, vol. J65-C, pp. 914-920, 1982.

[8] P. G. LeComber and W. E. Spear, "Doped amorphous semiconductors," in *Amorphous Semiconductors*, M. H. Brodsky, Ed. New York: Springer, 1979, p. 265.

[9] T. Tiedje, J. M. Cebulka, D. L. Morel, and B. Abeles, "Evidence for exponential band tails in amorphous silicon hydride," *Phys. Rev. Lett.*, vol. 46, pp. 1425-1428, 1981.

[10] S. Kishida, Y. Naruke, Y. Uchida, and M. Matsumura, "Theoretical analysis of amorphous-silicon field-effect transistors," *Japan. J. Appl. Phys.*, vol. 22, pp. 511-517, 1983.

Charge-Control Analysis of Class E Tuned Power Amplifier with Only One Inductor and One Capacitor in Load Network

MARIAN KAZIMIERCZUK

Abstract—**The following paper presents the charge-control analysis of operation of the transistor as a switch in the inverter circuit in which the collector current is constant while the transistor is saturated. This paper presents the charge-control analysis of the class E high-efficiency switching-mode tuned power amplifier with only 1 inductor and 1 capacitor in the load network, along with experimental results. In this amplifier, the collector current increases linearly with time while the transistor is saturated. We assume linear charge parameters of the transistor, and rectangular-wave base-drive current. The following are determined: the waveforms of all components of the base current and the base stored charge, the switching times, the driving power, and the power gain. A new definition of the overdrive factor of the transistor is introduced and the condition of the transistor saturation is discussed. It is shown that the base current necessary to drive the transistor to the edge of saturation increases with frequency f for $f > f_\beta$.**

Manuscript received January 4, 1983; revised September 20, 1983.

The author is with the Department of Electronics, Institute of Radioelectronics, Technical University of Warsaw, 00-665 Warsaw, Poland.

I. Introduction

THE CLASS E switching-mode tuned power amplifiers and oscillators [1]-[8] offer very high collector efficiency, typically, of the order of 96 percent. We achieve such high efficiency by shaping the collector voltage and current wave forms so as to minimize power losses in the transistor [3], [6], [7]. A recent publication [1] described one type of these circuits, named "class E amplifier with only 1 inductor and 1 capacitor in the load network," and another paper [2] presented an exact analysis of the amplifier.

The charge-control model of the bipolar transistor [9]-[25] has been applied previously to analyze the behavior of the transistor which operates as a switch in the inverter circuit having a load resistance R_L [26]-[34]. In that circuit, the collector current has a constant value $I_{C\,(sat)} \approx V_{CC}/R_L$ while the transistor is saturated. In the class E tuned power ampli-

0018-9383/84/0300-0366$01.00

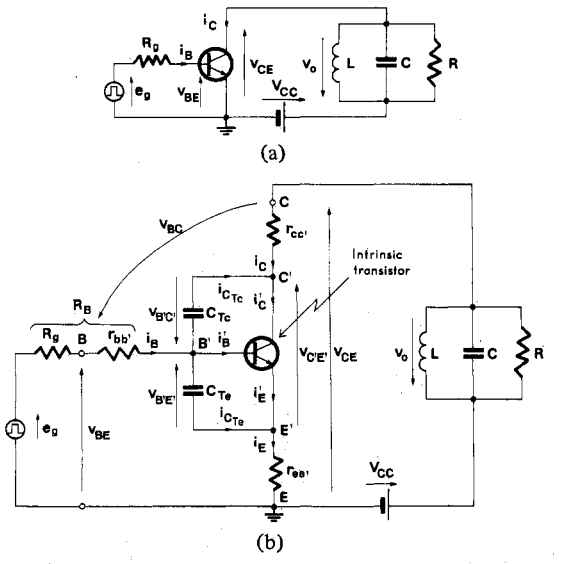

Fig. 1. Class E amplifier with only one inductor and one capacitor in the load network. (a) Basic circuit. (b) Equivalent circuit.

fier with only 1 inductor and 1 capacitor in the load network [1], [2], the collector current increases linearly with time while the transistor is saturated. That places a different requirement on the base drive needed to ensure proper circuit operation. This paper presents the charge-control analysis of the amplifier, along with experimental results.

II. Model of Class E Amplifier for Charge Analysis

Fig. 1(a) and (b) shows the basic circuit of the class E tuned power amplifier with only 1 inductor and 1 capacitor in the load network, and its equivalent circuit, respectively. The actual transistor consists of the intrinsic transistor, the junction transition (depletion-layer) capacitances C_{Te} and C_{Tc}, and the spreading resistances $r_{ee'}$, $r_{cc'}$, and $r_{bb'}$. Fig. 2 shows the idealized waveforms of the input and output currents and voltages. The waveforms of the base current i_B and the intrinsic base-to-emitter voltage $v_{B'E'}$[1] shown in Fig. 2(a) and (b) are valid for current-source drive of the transistor when it is in the saturation and active regions, i.e., for sufficiently high e_g and R_g. The waveforms of the collector current i_C and the collector-to-emitter voltage V_{CE} shown in Fig. 2(c) and (d) are valid for optimum operation of the amplifier [2]. Fig. 2 also shows all time intervals of operation of the transistor during 1 cycle. The turn-on switching time consists only of the delay time t_d. There is no "rise time" transient at turn-on in the same sense as in the inverter circuit which has a rectangular-waveform collector current. In this circuit, i_C starts at zero and has finite slope determined by the external circuit [3], [6]. The transistor is in the cutoff region during t_d. It is saturated during the time interval $0 < \omega t \leq 2\pi D$. The turn-off switching time consists of the storage time t_s and the fall time t_f. The transistor is in the saturation region during t_s and in the active-normal region during t_f. It is in the cutoff region after t_f.

[1] In power amplifiers, the terminal transitor currents are very high. Therefore, the external base-to-emitter voltage v_{BE} is substantially higher than the internal base-to-emitter voltage $v_{B'E'}$ because of the voltage drops across the spreading resistances $r_{ee'}$ and $r_{bb'}$.

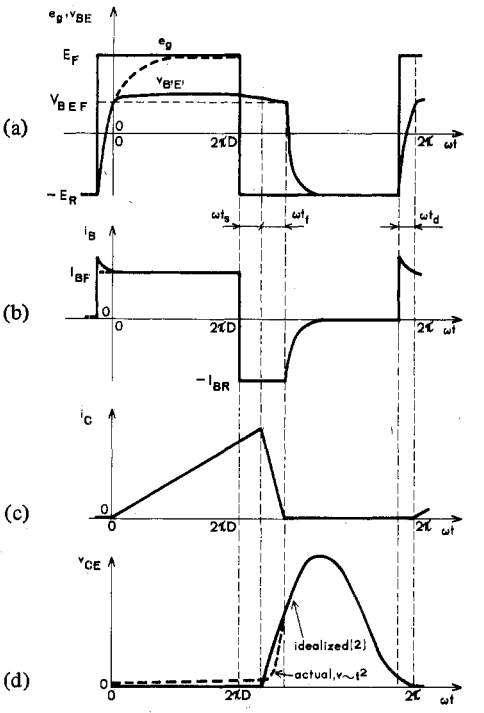

Fig. 2. Idealized waveforms of the input and output currents and voltages in the class E amplifier of Fig. 1.

The charge analysis of the amplifier is based on the following assumptions:

1) The large-signal charge parameters of the transistor h_{FE}, f_T, and τ_s are linear, i.e., they are constants.

2) The junction capacitances C_{Te} and C_{Tc} are linear.

3) The waveform of e_g is ideally rectangular, i.e., its rise and fall times are zero as shown in Fig. 2(a), and R_g is high enough that the transistor is driven from current source when it is in the saturation and active regions.

Later analyses here will use the waveform of i_C derived at $t_s = 0$ and $t_f = 0$ [2]

$$i_C(\omega t) = \begin{cases} \dfrac{I_{CM}}{2\pi D}\,\omega t = \dfrac{I_{CC}}{\pi D^2}\,\omega t, & \text{for} \quad 0 < \omega t \leq 2\pi D, \\ 0, & \text{for} \quad 2\pi D < \omega t \leq 2\pi \end{cases} \tag{1}$$

where $I_{CM} = i_C(2\pi D)$ is the peak collector current and $I_{CC} = DI_{CM}/2$ is the dc supply current. In actual amplifier, I_{CM} can be increased due to t_s, i.e., $I_{CM} = i_C(2\pi D + \omega t_s)$, and I_{CC} can be increased due to t_s and t_f, i.e., $I_{CC} = I_{CM}(2\pi D + \omega t_s + \omega t_f)/4\pi$, as shown in Fig. 2(c). However, t_s and t_f are not known *a priori*.

III. Time Interval of Transistor Saturation

A. Waveforms of Base Currents and Base Stored Charges

The transistor is saturated during the time interval $0 < \omega t \leq 2\pi D$. The base current is

$$i_B = I_{BF} = \frac{E_F - V_{BEF}}{R_B} \geq I_{BF\,\min} \tag{2}$$

where $R_B = R_g + r_{bb'}$, V_{BEF} is the threshold base-to-emitter voltage (≈ 0.75 V for silicon transistors), and $I_{BF\,\min}$ is the forward base current which is necessary to drive the transistor to the edge of saturation; this current is determined in Section III-B.

According to Fig. 1(b), the base current is

$$i_B(\omega t) = i'_B(\omega t) + i_{C_{Te}}(\omega t) + i_{C_{Te}}(\omega t). \tag{3}$$

Assuming that $v_{B'E'} = V_{BEF}$ and $v_{B'C'} = v_{B'E'} - v_{C'E'} = V_{BEF} - V_{C'E'\,(\mathrm{sat})}$ are constant, the currents through C_{Te} and C_{Tc} are

$$i_{C_{Te}}(t) = C_{Te}\frac{dv_{B'E'}(t)}{dt} = 0 \tag{4}$$

$$i_{C_{Tc}}(t) = C_{Tc}\frac{dv_{B'C'}(t)}{dt} = 0. \tag{5}$$

Hence, $i'_B = i_B = I_{BF}$ and $i'_C = i_C$.

The base current of the saturated intrinsic transistor is given by the expression

$$i_B(t) = i_{BS}(t) + i_{BX}(t) \tag{6}$$

in which

$$i_{BS}(t) = \frac{Q_{BS}(t)}{\tau_B} + \frac{dQ_{BS}(t)}{dt} = \frac{i_C(t)}{h_{FE}} + \frac{1}{\omega_T}\frac{di_C(t)}{dt} \tag{7}$$

$$i_{BX}(t) = \frac{Q_{BX}(t)}{\tau_S} + \frac{dQ_{BX}(t)}{dt} \tag{8}$$

where Q_{BS} is the base stored charge necessary to drive the transistor to the edge of saturation, Q_{BX} is the excess base stored charge, $\tau_B = 1/\omega_\beta = h_{FE}/\omega_T$ is the lifetime of Q_{BS}, τ_S is the lifetime of Q_{BX}, h_{FE} is the forward common-emitter dc current gain (I_C/I_B) at V_{CE} = const, and $f_T = \omega_T/2\pi$ is the gain-bandwidth product at V_{CE} = const.

From (1) and (7), base current necessary to drive the transistor to the edge of saturation is

$$i_{BS}(\omega t) = \frac{I_{CC}}{\pi D^2}\left(\frac{\omega t}{h_{FE}} + \frac{\omega}{\omega_T}\right). \tag{9}$$

Fig. 3(a) and (b) shows the waveforms of i_C, i_B, and i_{BS}. The second term in (9) increases with frequency; this effect has *an essential influence* on the behavior of the transistor with frequency. The peak values of both components in (9) become equal to each other at the frequency $f_{eq} = 2\pi D f_T/h_{FE} = 2\pi D f_\beta$. For $D = 0.5$, $f_{eq} = \pi f_T/h_{FE} = \pi f_\beta$.

From (2), (6), and (9), the excess base current is

$$i_{BX}(\omega t) = I_{BF} - i_{BS}(\omega t) = I_{BF} - \frac{I_{CC}}{\pi D^2}\left(\frac{\omega t}{h_{EF}} + \frac{\omega}{\omega_T}\right) \tag{10}$$

shown in Fig. 3(c).

Using (1), we obtain the base stored charge necessary to drive the transistor to the edge of saturation

$$Q_{BS}(\omega t) = \frac{i_C(\omega t)}{\omega_T} = \frac{I_{CC}}{\pi D^2 \omega_T}\omega t \tag{11}$$

shown in Fig. 3(d). We can also obtain the same result from (7) and (9).

Substitution of (10) into (8) and solution of the differential equation yields the excess base stored charge

$$Q_{BX}(\omega t) = \tau_S\left\{\left[I_{BF} + \frac{I_{CC}}{\pi D^2}\left(\frac{\omega\tau_S}{h_{FE}} - \frac{\omega}{\omega_T}\right)\right]\cdot\left(1 - e^{-\omega t/\omega\tau_S}\right) - \frac{I_{CC}\omega t}{\pi D^2 h_{FE}}\right\} \tag{12}$$

shown in Fig. 3(e).

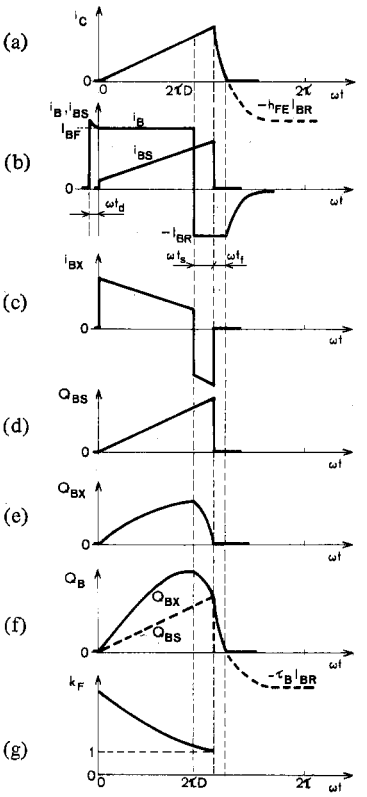

Fig. 3. Waveforms of the collector and base currents, the base stored charges, and the overdrive factor.

The total base stored charge is

$$Q_B(\omega t) = Q_{BS}(\omega t) + Q_{BX}(\omega t) \tag{13}$$

shown in Fig. 3(f).

B. Condition of Transistor Saturation

The condition of the transistor saturation is given by $Q_{BX}(\omega t) > 0$. If the collector current changes with time while the transistor is saturated, a new definition of the overdrive factor is needed. In this paper, the following definition of the overdrive factor is proposed

$$k_F(\omega t) = \frac{Q_B(\omega t)}{Q_{BS}(\omega t)} = 1 + \frac{Q_{BX}(\omega t)}{Q_{BS}(\omega t)}. \tag{14}$$

This factor is a measure of the depth of the transistor saturation.[2] The transistor is saturated if $k_F(\omega t) > 1$. It is at the edge of saturation at a given time instant t_0 if $k_F(\omega t_0) = 1$, i.e., $Q_{BX}(\omega t_0) = 0$. The depth of the transistor saturation increases

[2] In general, the overdrive factor given by (14) is a measure of the depth of the transistor saturation under dynamic conditions, i.e., 1) $i_C = f(t)$, and/or 2) $i_B = f(t)$, or 3) i_C = const, i_B = const, and $2\pi D < 4.6\,\tau_S$.

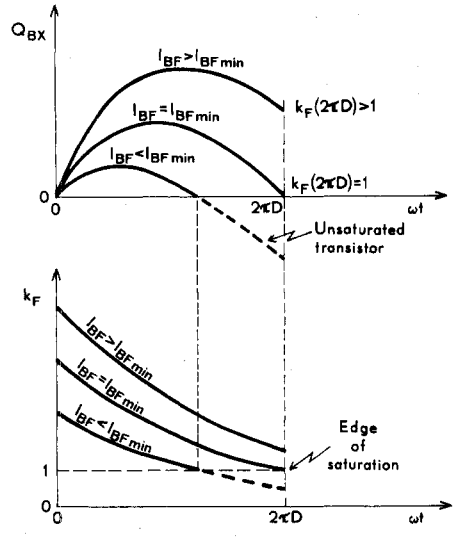

Fig. 4. Waveforms of the excess base stored charge Q_{BS} and the overdrive factor k_F at three values of forward base current I_{BF}.

with time if $dk_F(\omega t)/d(\omega t) > 0$, and decreases with time if $dk_F(\omega t)/d(\omega t) < 0$.

Substitution of (11) and (12) into (14) yields $k_F(\omega t)$ which is plotted in Fig. 3(g). It is seen that the depth of the transistor saturation decreases during the entire time interval $0 < \omega t \leqslant 2\pi D$.

The maximum value of k_F occurs at $\omega t = 0+$

$$k_F(0+) = \lim_{\omega t \to 0+} k_F(\omega t) = \frac{I_{BF}}{I_{CC}} \frac{\pi D^2 \omega_T}{\omega}. \tag{15}$$

This relationship shows that the transistor passes from the cutoff region to the saturation region, without passing through the active region. The device is in the cutoff region at the end of the delay time t_d, i.e., at $\omega t = 0-$, and is in the saturation region after t_d, i.e., at $\omega t = 0+$. Furthermore, the transistor is in deep saturation at $\omega t = 0+$ because $k_F(0+)$ is very high. Therefore, there is no "rise time" transient at turn-on of the transistor in the amplifier. Hence, the switching power loss in the transistor associated with the off-to-on transition of the transistor is zero, yielding high collector efficiency. This confirms the optimum-operation conditions of the class E amplifier: $v_{CE}(0) = V_{CE(sat)}$ and $i_C(0) = 0$; to achieve $i_C(0) = 0$, the condition $dv_{CE}(\omega t)/d(\omega t) = 0$ at $\omega t = 0$ must be fulfilled (Fig. 2 (c) and (d)). These conditions were discussed in detail in [3], [6] and utilized in [1], [2].

Fig. 4 shows Q_{BX} and k_F for three values of I_{BF}: "more than enough," "just enough," and "insufficient."

From (11), (12), and (14), I_{BF} required to obtain a given value of $k_F(2\pi D)$ is

$$I_{BF} = \frac{I_{CC}}{\pi D^2} \left\{ \frac{1}{h_{FE}} \left(\frac{2\pi D}{1 - e^{-2\pi D/\omega\tau_S}} - \omega\tau_S \right) + \frac{\omega}{\omega_T} + \frac{2[k_F(2\pi D) - 1]}{D\omega_T\tau_S(1 - e^{-2\pi D/\omega\tau_S})} \right\}. \tag{16}$$

Fig. 5 illustrates I_{BF}/I_{CC} as a function of f at $k_F(2\pi D) = 1$, 1.5, and 2 for $D = 0.5$, $h_{FE} = 97$, $f_T = 170$ MHz, and $\tau_S = 164$ ns. The characteristic frequencies are: $f_S = 1/2\pi\tau_S = 0.97$ MHz, $f_\beta = 1.75$ MHz, $f_{eq} = 5.5$ MHz, and $f_T = 170$ MHz. For $\omega << 1/\tau_S$

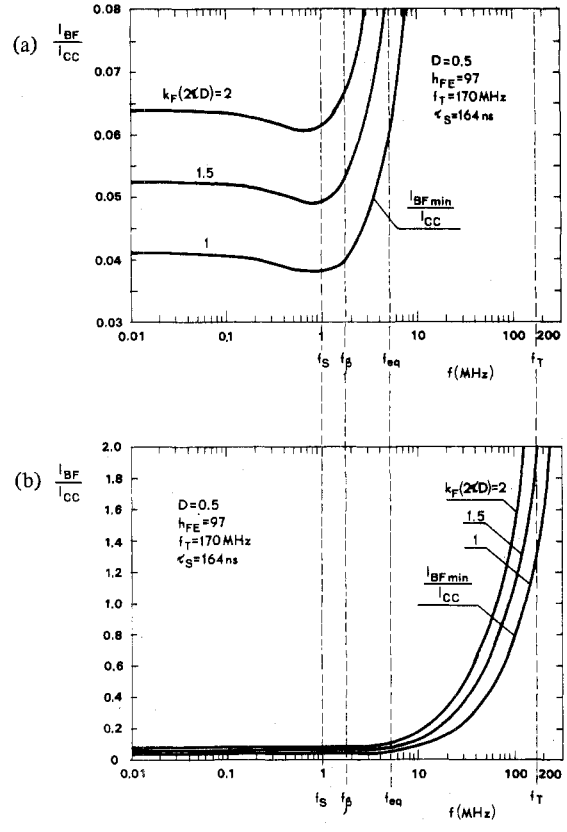

Fig. 5. Normalized forward base current I_{BF}/I_{CC} as a function of the operating frequency at three values of the overdrive factor $k_F(2\pi D)$. (a) At low frequencies. (b) In wide range of frequency.

$$I_{BF} \approx \frac{2I_{CC}}{D}\left[\frac{1}{h_{FE}} + \frac{k_F(2\pi D) - 1}{\pi D^2 \omega_T \tau_S}\right]. \tag{17}$$

For $\omega >> 1/\tau_S$

$$I_{BF} \approx \frac{I_{CC}}{\pi D^2} \frac{f}{f_T}\left[1 + \frac{k_F(2\pi D) - 1}{\pi D^2}\right]. \tag{18}$$

For $k_F(2\pi D) = 1$, the last term in (16) is zero and $I_{BF} = I_{BF\,min}$ (Fig. 4). $I_{BF\,min}/I_{CC}$ is shown in Fig. 5. For $\omega << 1/\tau_S$

$$I_{BF\,min} \approx \frac{2I_{CC}}{Dh_{FE}} \approx \frac{I_{CM}}{h_{FE}}. \tag{19}$$

In this case, $I_{BF\,min}$ is essentially independent of τ_S and ω_T. For $f > f_\beta$, $I_{BF\,min}/I_{CC}$ increases with frequency. For $\omega >> 1/\tau_S$

$$I_{BF\,min} \approx \frac{I_{CC}}{\pi D^2} \frac{f}{f_T} \approx \frac{I_{CM}}{2\pi D} \frac{f}{f_T}. \tag{20}$$

In this case, $I_{BF\,min}$ is essentially independent of h_{FE} and τ_S.

Fig. 6 shows variations in $I_{BF\,min}/I_{CC}$ with h_{FE}, f_T, and τ_S at three operating frequencies. $I_{BF\,min}/I_{CC}$ decreases with h_{FE} at each frequency (Fig. 6(a)). It is essentially independent of

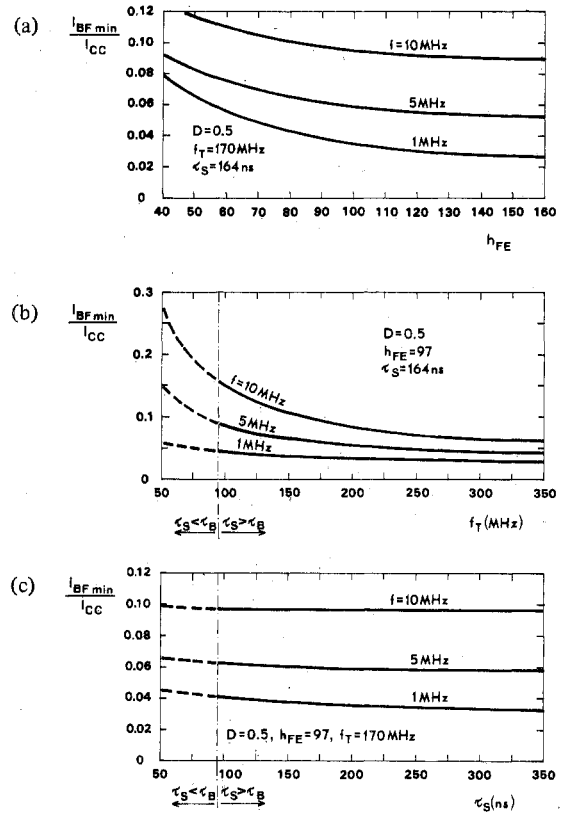

Fig. 6. Variations in the normalized minimum forward base current $I_{BF\,min}/I_{CC}$ with the transistor charge parameters. (a) $I_{BF\,min}/I_{CC}$ versus h_{FE}. (b) $I_{BF\,min}/I_{CC}$ versus f_T. (c) $I_{BF\,min}/I_{CC}$ versus τ_S.

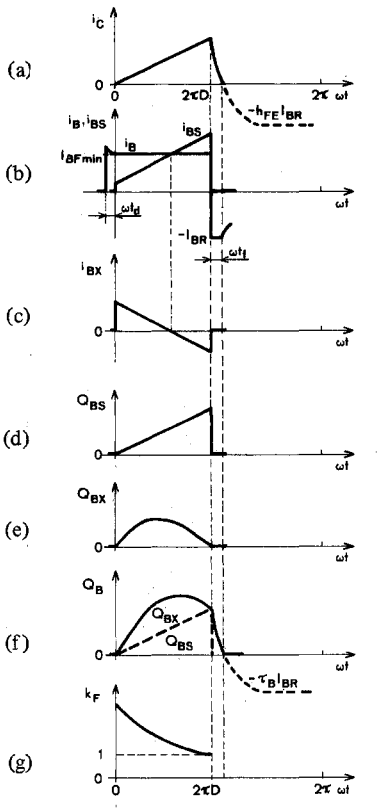

Fig. 7. Waveforms in the case of $k_F(2\pi D) = 1$.

f_T at low operating frequencies and decreases with f_T at high operating frequencies (Fig. 6(b)). It decreases slightly with τ_S (Fig. 6(c)). Since h_{FE} and f_T decrease with the dc collector current I_C in the range of its high values (τ_S increases with the collector current $I_{C\,(sat)}$ in saturation, but its influence is low), they should be evaluated at $I_C = I_{CM}$ to determine properly $I_{BF\,min}$. Moreover, h_{FE} and f_T increase with the dc collector-to-emitter voltage V_{CE}. Therefore, they should be determined at a low value of V_{CE}, e.g., at V_{CE} = 3 V.

For $I_{BF} = I_{BF\,min}$, the storage time $t_s = 0$ because $Q_{BX}(2\pi D) = 0$, i.e., $k_F(2\pi D) = 1$. Fig. 7 shows the waveforms in this case. Note that $i_{BS} > I_{BF}$ and $i_{BX} < 0$ during a significant time interval. In principle, it is possible to eliminate t_s. In practice, of course, this requires individual adjustment of "on" drive for each transistor and compensation for temperature changes.

IV. Storage Time

During the storage time $t_s (2\pi D < \omega t \leq 2\pi D + \omega t_s)$, the inverse base current is

$$i_B = -I_{BR} = -\frac{E_R + V_{BEF}}{R_B}. \tag{21}$$

The transistor is still saturated. Therefore, i_C, i_{BS}, and Q_{BS} determined by (1), (9), and (11) are valid; they are shown in Fig. 3(a), (b), and (d), respectively.

From (9) and (21), the excess base current is

$$i_{BX}(\omega t) = -I_{BR} - i_{BS}(\omega t) = -\left[I_{BR} + \frac{I_{CC}}{\pi D^2}\left(\frac{\omega t}{h_{FE}} + \frac{\omega}{\omega_T}\right)\right] \tag{22}$$

shown in Fig. 3(c).

Using (8) and (22), we can derive the excess base stored charge

$$Q_{BX}(\omega t) = Q_{BX}(2\pi D)\, e^{-(\omega t - 2\pi D)/\omega\tau_S} - \tau_S \left\{\left[I_{BR} - \frac{I_{CC}}{\pi D^2}\left(\frac{\omega\tau_S}{h_{FE}} - \frac{\omega}{\omega_T}\right)\right] \cdot \left[1 - e^{-(\omega t - 2\pi D)/\omega\tau_S}\right] + \frac{I_{CC}(\omega t - 2\pi D)}{\pi D^2 h_{FE}}\right\} \tag{23}$$

where $Q_{BX}(2\pi D)$ can be calculated from (12). Fig. 3(e) shows the waveform of Q_{BX}.

Substitution of (11) and (23) into (13) and (14) yields Q_B and k_F, respectively; they are shown in Fig. 3(f) and (g).

The storage time t_s is determined by $Q_{BX}(2\pi D + \omega t_s) = 0$ Hence, from (23)

$$Q_{BX}(2\pi D)\, e^{-t_s/\tau_S} - \tau_S \left\{\left[I_{BR} - \frac{I_{CC}}{\pi D^2}\left(\frac{\omega\tau_S}{h_{FE}} - \frac{\omega}{\omega_T}\right)\right] \cdot \left(1 - e^{-t_s/\tau_S}\right) + \frac{I_{CC}\omega\tau_S}{\pi D^2 h_{FE}}\right\} = 0. \tag{24}$$

The storage time t_s can be computed from the above equation only numerically. For $t_s \ll \tau_S$

TABLE I
COMPARISON OF VALUES OF t_s CALCULATED FROM (24) AND (25); $h_{FE} = 97$, $f_t = 170$ MHz, $\tau_S = 164$ ns, $D = 0.5$, $I_{CC} = 192$ mA $I_{BR} = 40$ mA, $Q_{BX}(2\pi D) = 0.3595$ nC AT $k_F(2\pi D) = 1.5$, AND $Q_{BX}(2\pi D) = 0.719$ nC AT $k_F(2\pi D) = 2$

f(MHz)	$k_F(2\pi D)$ = 1.5			$k_F(2\pi D)$ = 2		
	t_s (ns) from (24)	t_s (ns) from (25)	% difference	t_s (ns) from (24)	t_s (ns) from (25)	% difference
1	8.44	8.24	-2.37	16.44	15.69	-4.56
1.75	8.22	8.04	-2.19	16.01	15.33	-4.25
5.5	7.29	7.18	-1.51	14.18	13.75	-3.03
10	6.42	6.35	-1.09	12.49	12.24	-2.00
15	5.68	5.64	-0.70	11.05	10.90	-1.36
20	5.09	5.07	-0.39	9.92	9.83	-0.91

$$t_s \approx \frac{Q_{BX}(2\pi D)}{I_{BR} + \dfrac{I_{CC}\omega}{\pi D^2 \omega_T} + \dfrac{Q_{BX}(2\pi D)}{\tau_S}}. \tag{25}$$

Table I shows the values of t_s calculated from (24) and (25).

V. Fall Time

During the collector-current fall time $t_f (2\pi D + \omega t_s < \omega t \leqslant 2\pi D + \omega t_s + \omega t_f)$, the transistor is in the active-normal region and acts as a current source. The voltage $v_{B'E'} \approx V_{BEF}$. Hence, from (4), $i_{C_{Te}} \approx 0$. Neglecting the feedback via C_{Tc}, $i_B = i'_B = -I_{BR}$ and $i_C = i'_C$. The base current is

$$i_B(t) = -I_{BR} = \frac{i_C(t)}{h_{FE}} + \frac{1}{\omega_T}\frac{di_C(t)}{dt}. \tag{26}$$

Hence, we obtain the collector current

$$i_C(\omega t) = (I_{CM} + h_{FE} I_{BR})\, e^{-(\omega t - 2\pi D - \omega t_s)/\omega\tau_B} - h_{FE} I_{BR} \tag{27}$$

shown in Fig. 3(a).

The base stored charge is

$$Q_B(\omega t) = \frac{i_C(\omega t)}{\omega_T} = \left(\frac{I_{CM}}{\omega_T} + \tau_B I_{BR}\right) \cdot e^{-(\omega t - 2\pi D - \omega t_s)/\omega\tau_B} - \tau_B I_{BR} \tag{28}$$

shown in Fig. 3(f).

The fall time t_f is determined by $i_C(2\pi D + \omega t_s + \omega t_f) = 0$. Hence, from (27)

$$t_f = \tau_B \ln\left(1 + \frac{I_{CM}}{h_{FE} I_{BR}}\right) = \frac{h_{FE}}{\omega_T} \ln\left(1 + \frac{I_{CM}}{h_{FE} I_{BR}}\right). \tag{29}$$

The maximum operating frequency of the amplifier is determined by $2\pi D + \omega(t_s + t_f) = 2\pi$. Hence

$$f_{\max} = \frac{1 - D}{t_s + t_f}. \tag{30}$$

For $t_s = 0$, this reduces to $f_{\max} = (1 - D)/t_f$.

VI. Input Power and Power Gain

The input (driving) power is

$$P_{\text{in}} = \frac{1}{2\pi}\int_0^{2\pi} i_B v_{BE}\, d(\omega t) \approx P_{\text{on}} + P_{t_{sf}} \tag{31}$$

where

$$P_{\text{on}} = D I_{BF} V_{BEF} \tag{32}$$

$$P_{t_{sf}} = -f(t_s + t_f) I_{BR} V_{BEF}. \tag{33}$$

Here, we can assume that V_{BEF} is of the order of 1 V because of the voltage drops across $r_{ee'}$ and $r_{bb'}$. Substitution of (16) into (32) yields the required power P_{on}. For $\omega \ll 1/\tau_S$, using (17) and (32)

$$P_{\text{on}} \approx 2 V_{BEF} I_{CC}\left[\frac{1}{h_{FE}} + \frac{k_F(2\pi D) - 1}{\pi D^2 \omega_T \tau_S}\right]. \tag{34}$$

For $\omega \gg 1/\tau_S$, using (18) and (32)

$$P_{\text{on}} \approx \frac{V_{BEF} I_{CC} f}{\pi D^2 f_T}\left[1 + \frac{k_F(2\pi D) - 1}{\pi D^2}\right]. \tag{35}$$

It is seen that P_{on} increases with frequency at high frequencies. Substituting $k_F(2\pi D) = 1$ into (34) and (35), we obtain the minimum required power $P_{\text{on min}}$.

The power gain is

$$k_p = \frac{P_{\text{out}}}{P_{\text{in}}} \tag{36}$$

where P_{out} is the output power. Since the collector efficiency $\eta_C \approx 1$ [1], [2], $P_{\text{out}} \approx P_{CC} = I_{CC} V_{CC}$. Hence, $k_p \approx P_{CC}/P_{\text{in}}$. For $\omega \ll 1/\tau_S$, neglecting $P_{t_{sf}}$ and using (34)

$$k_p \approx \frac{P_{\text{out}}}{P_{\text{on}}} \approx \frac{V_{CC}}{V_{BEF}} \frac{1}{2\left[\dfrac{1}{h_{FE}} + \dfrac{k_F(2\pi D) - 1}{\pi D^2 \omega_T \tau_S}\right]}. \tag{37}$$

For $k_F(2\pi D) = 1$, we obtain the maximum power gain

$$k_{p\max} \approx \frac{P_{\text{out}}}{P_{\text{on min}}} \approx \frac{V_{CC}}{V_{BEF}} \frac{h_{FE}}{2}. \tag{38}$$

For $\omega \gg 1/\tau_S$, the power gain obtained from (31), (32), (33), (35), and (36) is

$$k_p = \frac{P_{\text{out}}}{P_{\text{in}}} \approx \frac{V_{CC}}{V_{BEF}} \cdot \frac{1}{f\left\{\dfrac{1}{\pi D f_T}\left[1 + \dfrac{k_F(2\pi D) - 1}{\pi D^2}\right] - \dfrac{(t_s + t_f) I_{BR}}{I_{CC}}\right\}}. \tag{39}$$

For $k_F(2\pi D) = 1$, we obtain the maximum power gain

$$k_{p\max} = \frac{P_{\text{out}}}{P_{\text{in min}}} \approx \frac{V_{CC}}{V_{BEF}} \frac{1}{f\left(\dfrac{1}{\pi D f_T} - \dfrac{t_f I_{BR}}{I_{CC}}\right)}. \tag{40}$$

It is seen that k_p and $k_{p\max}$ decrease with frequency at high frequencies.

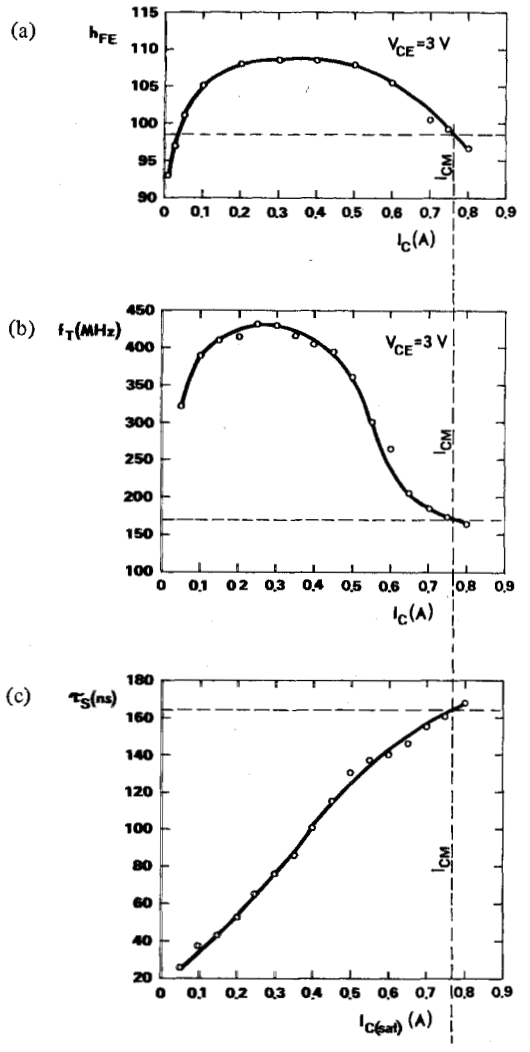

Fig. 8. Measured charge parameters of a BSX60 transistor. (a) h_{FE} versus I_C. (b) f_T versus I_C. (c) τ_S versus $I_{C\,(sat)}$.

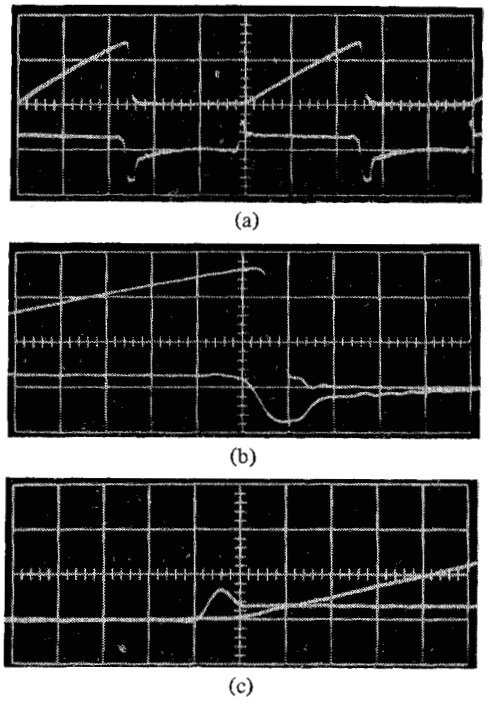

Fig. 9. Waveforms of i_C and i_B. (a) i_C and i_B. (b) i_C and i_B during turn-off of the transistor. (c) i_C and i_B during turn-on of the transistor. Horizontal: (a) 200 ns/div.; (b) and (c) 40 ns/div.; vertical: i_C, 540 mA/div. and i_B, 27 mA/div.

VII. Experimental Results

Fig. 8 shows the charge parameters of a BSX60 transistor, measured by methods given in [35], [36]. The peak collector current I_{CM} was 768 mA in the amplifier circuit of Fig. 1(a) designed in [2]. In accordance with the discussion in Section III-B, h_{FE} and f_T were measured at V_{CE} = 3 V. From Fig. 8, the transistor charge parameters are: h_{FE} = 97 and f_T = 170 MHz at $I_C = I_{CM}$, and τ_S = 164 ns at $I_{C\,(sat)} = I_{CM}$. They were used in the previous analysis.

Experiments were carried out in the circuit of Fig. 1(a), using a BSX60 transistor, D = 0.5, f = 1 MHz, and R_B = 254 Ω. The waveforms of i_C and i_B are shown in Fig. 9(a). Fig. 9(b) and (c) shows the same waveforms during turn-off and turn-on of the transistor, with an enlarged time-scale. They agree well with the theoretical waveforms of Fig. 3(a) and (b).

The calculated $I_{BF\,min}$ was 7.15 mA and the measured value was 6.6 mA. In this case, t_s was approximately zero.

VIII. Conclusions

1) A measure of the depth of the transistor saturation under dynamic conditions (i.e., i_C and/or i_B changes with time while the transistor is saturated) can be the charge overdrive factor defined by (14).

2) The minimum forward base current $I_{BF\,min}$ necessary to drive the transistor to the edge of saturation increases with frequency f for $f > f_\beta$.

3) The base current i_{BS} necessary to drive the transistor to the edge of saturation can be higher than the total forward base current I_{BF} if the collector current changes with time while the transistor is saturated (Fig. 7).

4) The charge-control analysis confirms the previous papers [3], [6] that there is no "rise time" transient at turn-on of the transistor in the class E amplifier; the device passes from the cutoff region to the saturation region, without passing through the active region.

5) The storage time t_s can be reduced approximately to zero in the class E amplifier of Fig. 1(a), but this may require individual adjustment of "on" base drive and compensation for temperature changes.

The presented method of the charge-control analysis can be applied to other switching circuits in which the collector current changes with time while the transistor is saturated. Examples of such circuits are other types of the class E amplifiers, class D amplifiers, and switching-mode power converters.

References

[1] N. O. Sokal, "Class E high-efficiency switching-mode tuned power amplifier with only one inductor and one capacitor in load network—Approximate analysis," *IEEE J. Solid-State Circuits*, vol. SC-16, pp. 380–384, Aug. 1981.

[2] M. Kazimierczuk, "Exact analysis of class E tuned power amplifier with only one inductor and one capacitor in load network," *IEEE J. Solid-State Circuits*, vol. SC-18, pp. 214–221, Apr. 1983.

[3] N. O. Sokal and A. D. Sokal, "Class E–A new class of high-efficiency tuned single-ended switching power amplifiers," *IEEE J. Solid-State Circuits*, vol. SC-10, pp. 168–176, June 1975.
[4] F. H. Raab, "Idealized operation of the class E tuned power amplifier," *IEEE Trans. Circuits Syst.*, vol. CAS-24, pp. 725–735, Dec. 1977.
[5] —, "Effects of circuit variations on the class E tuned power amplifier," *IEEE J. Solid-State Circuits*, vol SC-13, pp. 239–247, Apr. 1978.
[6] M. Kazimierczuk, "Theory of the class E tuned power amplifier" (in Polish), *Rozprawy Elektrotechniczne*, vol. 25, no. 4, pp. 957–986, 1979.
[7] —, "Class E tuned power amplifier with shunt inductor," *IEEE J. Solid-State Circuits*, vol. SC-16, pp. 2–7, Feb. 1981.
[8] J. Ebert and M. Kazimierczuk, "Class E high-efficiency tuned power oscillator," *IEEE J. Solid-State Circuits*, vol. SC-16, pp. 62–66, Apr. 1981.
[9] R. Beaufoy and J. J. Sparkes, "The junction transistor as a charge-controlled device," *A. T. E. Journal*, vol. 13, pp. 310–327, Oct. 1957.
[10] —, "The junction transistor as a charge controlled device," *Proc. IRE*, vol. 45, pp. 1740–1742, Dec. 1957.
[11] L. J. Varnerin, "Stored charge method of transistor base transit analysis," *Proc. IRE*, vol. 47, pp. 523–527, Apr. 1959.
[12] A. N. Baker, "Charge analysis of transistor operation," *Proc. IRE*, vol. 48, pp. 949–950, May 1960.
[13] A. N. Baker and W. G. May, "Charge analysis of transistor operation including delay effects," *IRE Trans. Electron Devices*, vol. ED-8, pp. 152–154, Mar. 1961.
[14] J. J. Sparkes, "The measurement of transistor transient switching parameters," *Proc. IEE*, pt. B, vol. 106, suppl. 15, pp. 562–567, May 1959.
[15] R. Beaufoy, "Transistor switching circuit design in terms of charge parameters," *Proc. IEE*, pt. B, vol. 106, suppl. 17, pp. 1085–1091, May 1959.
[16] A. Kruithof, "Transient response of junction transistors and its graphical representation," *Proc. IEE*, pt. B, vol. 106, suppl. 17, pp. 1092–1101, May 1959.
[17] J. J. Sparkes, "A study of the charge control parameters of transistors," *Proc. IRE*, vol. 48, pp. 1696–1705, Oct. 1960.
[18] E. D. Hooper and A. R. T. Turnbull, "Applications of the charge-control concept to transistor characterization," *Proc. IRE* (Australia), vol. 23, pp. 132–147, Mar. 1962.
[19] D. J. Hamilton, F. A. Lindholm, and J. A. Narud, "Comparison of large signal models for junction transistors," *Proc. IEEE*, vol. 52, pp. 239–248, Mar. 1964.
[20] D. Koehler, "The charge-control concept in the form of equivalent circuits, respresenting a link between the classic large signal diode and transistor models," *Bell Syst. Tech. J.*, vol. 46, pp. 523–576, Mar. 1967.
[21] H. K. Gummel and H. C. Poon, "An integral charge control model of bipolar transistors," *Bell Syst. Tech. J.*, vol. 49, pp. 827–852, May/June 1970.
[22] H. K. Gummel, "A charge control relation for bipolar transistors," *Bell Syst. Tech. J.*, vol 49, pp. 115–120, Jan. 1970.
[23] B. R. Chawla, "Circuit representation of the integral charge-control model of bipolar transistor," *IEEE J. Solid-State Circuits*, vol. SC-6, pp. 262–264, Aug. 1971.
[24] J. te Winkel, "Extended charge-control model for bipolar transistor," *IEEE Trans. Electron Devices*, vol. ED-20, pp. 389–394, Apr. 1973.
[25] N. O. Sokal, "RF power transistor storage time: Theory and measurements," *IEEE J. Solid-State Circuits*, vol SC-11, pp. 344–346, Apr. 1976.
[26] R. P. Nanavati, "Prediction of storage time in junction transistors," *IRE Trans. Electron Devices*, vol. ED-7, pp. 9–15, Jan. 1960.
[27] R. P. Nanavati and R. J. Wilfinger, "Predicting transistor storage time for nonstep, quasi-voltage inputs," *IRE Trans. Electron Devices*, vol. ED-9, pp. 491–499, Nov. 1962.
[28] R. P. Nanavati, "Charge control analysis of transistor storage time dependence on input "on" pulse width," *IRE Trans. Electron Devices*, vol. ED-10, pp. 290–291, July 1963.
[29] H. J. Kuno, "Rise and fall time calculations of junction transistors," *IEEE Trans. Electron Devices*, vol. ED-11, pp. 151–155, Apr. 1964.
[30] Y. Hsia, and F-H. Wang, "Switching waveform prediction of a simple transistor inverter circuit," *IEEE Trans. Electron Devices*, vol. ED-12, pp. 626–631, Dec. 1965.
[31] S. S. Hakim, *Junction Transistor Circuit Analysis.* London, England: Iliffe, 1962, ch. 11, pp. 392–417.
[32] P. E. Gray and C. E. Searle, *Electronic Principles; Physics, Models, and Circuits.* New York: Wiley, 1969, ch. 8.
[33] E. S. Yang, *Fundamentals of Semiconductor Devices.* New York: McGraw-Hill, 1978, ch. 9, pp. 248–252.
[34] P. L. Hower, "Application of a charge-control model to high-voltage power transistors," *IEEE Trans. Electron Devices*, vol. ED-23, pp. 863–870, Aug. 1976.
[35] I. E. Getreu, *Modeling the Bipolar Transistor.* Amsterdam, The Netherlends: Elsevier, 1978, ch. 3, pp. 169–178, also available from Tektronix, Inc. Field Offices (or Headquarters, Beaverton, OR 97077, U.S.A.), as Part no. 062-2841-00.
[36] M. Kazimierczuk, "Accurate measurement of lifetime of excess base stored charge at high collector currents," *IEEE Trans. Electron Devices*, vol. ED-31, no. 3, Mar. 1984.